ARCHIVES OF ELECTRICAL ENGINEERING VOL. 73(4), pp. 1047–1067 (2024)

DOI 10.24425/aee.2024.152110

Optimal control of grid-connected overvoltage of distributed photovoltaic power generation based on cluster division

JIANFENG YANG, TAO ZHOU✉, SHIKUN ZHU, CHENYANG JIA

School of Automation and Electrical Engineering, Lanzhou Jiaotong University
Lanzhou, China
e-mail: ✉ *11220384@stu.lzjtu.edu.cn*

(Received: 06.04.2024, revised: 22.11.2024)

Abstract: To address the overvoltage problem caused by the reverse flow of current when a high proportion of distributed photovoltaic (PV) is connected to the distribution network, this paper proposes a grid-connected voltage regulation control strategy based on the cluster division of the Distributed Model Predictive Control (DMPC) algorithm. Firstly, the overvoltage responsibility of each node is calculated using the Shapley value method. This is combined with k-means clustering to achieve effective cluster division, enabling dynamic adjustment of the active and reactive power of photovoltaic power generation units to stabilize regional voltage. Secondly, a group grid-connected voltage control strategy is introduced. This strategy controls the active and reactive power outputs by integrating real-time power output and voltage information from PV generating units in the region with the DMPC algorithm, ensuring overall voltage stability of the grid-connected system. Finally, actual overvoltage data from a 10 kV distribution line in the Dingxi power grid, Gansu Province, is used to verify that under the proposed control strategy, PV grid-connected overvoltage nodes are maintained within 1.06 p.u. The control effect is improved by a margin of 0.05 compared to traditional control methods. This demonstrates the effectiveness of the grouped grid-connected voltage regulation control strategy, achieving smoother voltage regulation performance in distributed PV grid-connected systems.

Key words: cluster division, distribution network, distributed photovoltaics, grid control, overvoltage

1. Introduction

1.1. Motivation and aims

With the emergence of global energy shortages, China has proposed a "dual-carbon" national strategic goal aimed at peaking carbon dioxide emissions by 2030 and achieving carbon neutrality by 2060. Increasing the share of new energy generation is pivotal in implementing the "dual-carbon" goal. This strategy also involves enhancing the proportion of non-fossil energy consumption, thereby facilitating the broader objective of energy transformation. [1].

According to China's National Energy Administration statistics on May 6, 2024, China's overall PV new grid-connected capacity in the first quarter of 2024 was a total of 4.5740 (MW); of which: centralized PV power plants – 2.1930 (MW); distributed PV - 2.3810 (MW) including household distributed – 6920 (MW). By the end of March 2024, the cumulative grid-connected capacity was 6595 (MW). Especially in Northwest China, light resources are abundant, and the PV industry is developing more rapidly. In the future, following the national strategy to accelerate the transformation of clean and low-carbon energy supply, it is inevitable to continue to vigorously develop new energy sources. However, the rapid development of distributed PV high penetration and PV power generation that is intermittent and fluctuating will cause the grid regulator control to face many challenges [2]. When there is a high penetration of PV in the distribution network, it exacerbates frequency and voltage fluctuations, thereby affecting the safe and stable operation of the distribution network. This can lead to issues with power balance, power quality on the user side, and the overall reliability of the power supply [3].

The main issues that may arise upon connecting to the network include voltage overruns, voltage imbalances, line overloading, flicker, and exceeding harmonic standards. Among these, overvoltage problems are typically the primary limiting factor for PV integration capacity. When a high proportion of distributed PV is connected to the distribution network, excessive midday sunlight can lead to PV generation surpassing user demand. In the absence of energy storage systems, this can cause reverse power flow, resulting in overvoltage issues within the distribution network [4]. Addressing distributed PV grid-connected point voltage regulation and control to limit overvoltage problems will be crucial for overcoming the primary limitations on PV development in the future. Currently, two primary grid-connected PV control methods are prevalent: centralized and decentralized [6]. Addressing the electricity supply shortage in Cameroon, Reference [10] constructs a procedural methodology for assessing installed solar PV capacity on the interconnected grid for dynamic analysis. It evaluates the technical stability of the grid against substantial disturbances under optimal solar PV penetration. Furthermore, Reference [11] proposes an optimal configuration of Phasor Measurement Units (PMUs) to tackle the dynamic stability issues of the Southern Interconnected Grid (SIG) in Cameroon, providing a system path for distributed solar PV generation to accommodate growing loads. The aforementioned reference focuses on the use of flexible power equipment.

This paper adopts an alternative perspective by employing intelligent control technology to enhance power system stability and concentrates on resolving the grid-connected over-voltage problem caused by photovoltaic access.

1.2. Literature review and identification of research gaps

In the field of overvoltage issues, current researchers primarily address the problem through three mainstream approaches:

1. configuring energy storage systems,
2. regulating reactive power in conjunction with limiting active power output, and
3. adjusting the tap switching position of on-load regulator transformers.

Reference [12] analyzes and studies the impact of smart transformers on various radial distribution systems. It introduces an improved backward/forward trending algorithm for the deployment of smart transformers in radial distribution systems. The direct trending method is utilized, focusing on the seamless integration of smart transformers with the grid and addressing grid updating challenges. The optimal configuration of smart transformers is optimized to minimize power losses in the grid. The effectiveness of the approach in addressing common grid issues using smart transformers is evaluated. However, the final solution necessitates frequent transformer operations, which may introduce new transient disturbances to the distribution grid. This aspect of transformer regulation grid integration has not been adequately addressed.

Neural networks and other adaptive algorithms for power control methods are also frequently mentioned. For example, Reference [13] utilizes a Back Propagation (BP) neural network prediction model, combining weather forecasts, light intensity, temperature, and real-time output power of PV power generation to predict the need to reduce active power and control PV power output to prevent overvoltage occurrences. This method requires processing a large amount of data, which is highly demanding, and the final prediction accuracy cannot be guaranteed to meet the required standards.

References [14] construct a mathematical model for optimal voltage regulation of energy storage by determining the power and state of charge (SOC) of the energy storage system. It allocates energy storage within the cluster based on the total power required by the cluster where the node with the overrun voltage is located, and determines the timing of storage actions to maximize the operating benefit of the distributed energy storage. The results show that the control scheme significantly limits voltage overruns. However, the high cost of current energy storage equipment makes it impractical to install such equipment at each PV point. Additionally, due to the complexity of the grid structure across the entire power sector, determining the reasonable capacity of energy storage installations remains a practical issue. Furthermore, the impact of this scheme on the overvoltage correlation between clusters is not considered.

References [16] consider the relevant constraints of different PV systems and loads within a specific region, linearizes the non-linear constraints, and ultimately establishes a distributed optimal dispatch model for active distribution networks to achieve efficient and optimal scheduling. The method of distributed optimization adopted can refine the problem of interest game among the stakeholders under operational constraints.

To address this issue, this paper undertakes cluster division control. Several prevalent approaches for cluster division optimization in current studies include the network division method proposed by Reference [19], which utilizes the k-means clustering algorithm. Additionally, intelligent heuristic algorithms such as the immunity algorithm [21] are frequently employed for cluster segmentation of distribution networks. Furthermore, there are multi-attribute cluster segmentation

approaches that integrate factors like geographic distances, line resistances, and loads. For instance, Reference [18] establishes a second-order conical optimization model to iteratively optimize through an active-reactive power partitioning approach, with an objective function aimed at minimizing regulation. Cluster division is performed based on the influence of active and reactive power on overvoltage control and corresponding indicators.

A summary of the contribution and novelty presented in this study are as follows:

- The Shapley value method, derived from cooperative game theory, is employed to quantify the overvoltage liability attributed to each PV node. This approach allows for the calculation and determination of output values, thereby addressing the issue of frequent inverter actions.
- Due to the complexity arising from numerous control variables, which leads to a computational dimensionality explosion, this paper integrates mainstream solutions with the k-means clustering method to achieve cluster division. This facilitates the dynamic adjustment of active and reactive power in PV power generation units. The proposed approach aims to stabilize regional voltage, maximize power utilization, and mitigate the issue of voltage overruns.
- The DMPC algorithm is employed on a cluster-based basis to regulate voltage control strategies following grid connection and address instances of voltage limit violations.

2. PV grid-connected overvoltage mechanism analysis

2.1. Nodal overvoltage liability calculation

The network wiring topology shown in Fig. 1 serves as an example to illustrate the mechanism of overvoltage generation when PV systems are grid-connected. In the distribution line depicted, divided into four regions at nodes $i/j/k+1$, there are two branches, with the three branch end nodes labeled F/N/R. Additionally, within the three branches and at node $i+2$, there are connections to the distributed PV systems.

According to the Distflow tidal equation [21], take branch 1 as an example to derive the voltage relationship between node n and the previous node n-1 as:

$$U_n^2 = U_{n-1}^2 - 2(P_n R_n + Q_n X_n) + (R_n^2 + X_n^2)\frac{P_n^2 + Q_n^2}{U_n^2}, \tag{1}$$

where: U_n and U_{n-1} are the voltages at node $n$and the previous node $n-1$, respectively; P_n and Q_n are the active and reactive power from the previous node to the next node, respectively; R_n and X_n are the resistance and impedance values between node $n$and the previous node, respectively. Since the third term of the three terms of the above equation is much smaller than the other two terms, the simplification gives:

$$U_n^2 = U_{n-1}^2 - 2(P_n R_n + Q_n X_n). \tag{2}$$

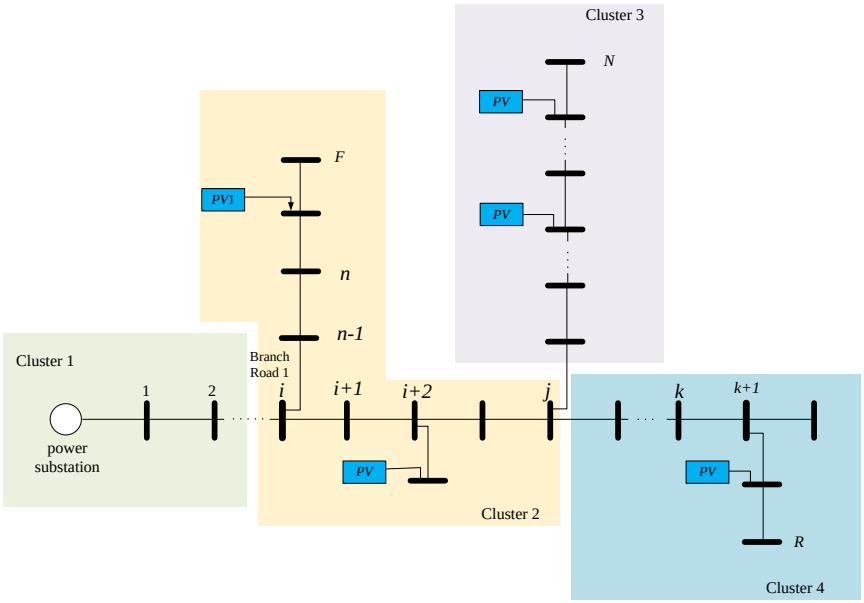

Fig. 1. Distribution network simplified topology

Superimposed on nodes above node n:

$$U_n^2 = U_{n-1}^2 - 2(P_n R_n + Q_n X_n) + 2\sum_{k=1}^{n} P_k R_k + Q_k X_k. \tag{3}$$

The above equation combined with the topology from Fig. 1 can be obtained:

$$P_2 = (P_{L2} - P_{G2}) + \sum_{n=3\text{free}dF}^{F} (P_{Ln} - P_{Gn}) + \sum_{n=3\text{free}dN}^{N} (P_{Ln} - P_{Gn}) + \sum_{n=3\text{free}dR}^{R} (P_{Ln} - P_{Gn}), \tag{4}$$

$$Q_2 = (Q_{L2} - Q_{G2}) + \sum_{n=3\text{free}dF}^{F} (Q_{Ln} - Q_{Gn}) + \sum_{n=3\text{free}dN}^{N} (Q_{Ln} - Q_{Gn}) + \sum_{n=3\text{free}dR}^{R} (Q_{Ln} - Q_{Gn}). \tag{5}$$

The single node i and k active reactive power are calculated as:

$$\begin{aligned} P_i &= \sum_{n=i}^{F} (P_{Ln} - Q_{Gn}), \quad Q_i = \sum_{n=i}^{F} (Q_{Ln} - Q_{Gn}), \\ P_k &= \sum_{n=k}^{F} (P_{Ln} - Q_{Gn}), \quad Q_k = \sum_{n=k}^{F} (Q_{Ln} - Q_{Gn}), \end{aligned} \tag{6}$$

where P_{Ln}, Q_{Ln}, P_{Gn}, Q_{Gn} ($n = 1, 2, 3, \ldots$) are the active load, reactive load and active reactive generation at node n, respectively.

Based on Eqs. (1)–(6), it is evident that the voltage at the PV grid-connected point is not solely contingent upon the output of the PV system itself. It is also influenced by the outputs of all

PV systems across other branch circuits and the entirety of the distribution system. Furthermore, as indicated by Eq. (3), the voltage at node n, in relation to the first node, is susceptible to the transmission power along its respective supply path. In instances where the distributed PV power exceeds the load demand, the reverse transmission power along the supply line will elevate the voltage at the grid-connected node, potentially leading to overvoltage issues.

In the case of increasing PV penetration; the main solutions to the overvoltage problem on PV distribution lines with high penetration are to reduce active power back-feeding on the line and to increase inductive reactive power flow in two ways. In distribution lines, local power control can effectively address overvoltage at a single node. However, the reactive capacity of a single node is constrained, and the influence of reactive power compensation both upstream and downstream of a node on a single line necessitates analysis. With increasing penetration, single node control exhibits limited suppression efficacy. Line voltage overvoltage often stems from the cumulative impact of PV power backflow across multiple nodes along the entire line. Consequently, the entirety of the distribution line is examined as a whole, employing cluster division and coordinated control units to tackle overvoltage issues comprehensively. The subsequent delineation outlines the specific criteria for cluster division and the distribution of responsibilities in the calculation process.

2.2. Nodal overvoltage liability calculation

The overvoltage generation in the actual distribution line stems from the cumulative effect of power backflow from all PV nodes. Therefore, by incorporating overvoltage generation into the responsibility calculation based on cluster division, adjustments for overvoltage across the entire distribution line can be comprehensively and accurately controlled. Within the same distribution system, which includes multiple PV nodes, the Shapley value calculation method from cooperative game theory is applied to ascertain the specific responsibility magnitude of each PV node in causing overvoltage.

When utilizing the Shapley value method [21] a crucial step involves defining the utility function, which, in the context of the overvoltage problem, is represented by the overvoltage index. Here, a weighted voltage deviation index, known as the load-weight voltage deviation index (LVDI), is considered. This index incorporates both the load size and the overall overvoltage level as the primary weighting factors.

$$\mathrm{LVDI}(H) = \sum_{i} \frac{U_{i,t} - U_{\max}}{U_{\max}} \tau_{i,t}(H), \tag{7}$$

where: LVDI(H) is the load deviation voltage weighted index at time t, $U_{i,t}$ is the voltage at node i at moment t, which is the upper voltage limit specified by the distribution network; H is the set of all nodes where overvoltage occurs, and $\tau_{i,t}(H)$ is the load node weights at that moment. The specific calculation is:

$$\tau_{i,t}(H) = \frac{\hat{P}_{i,t}}{\sum_{m} \hat{P}_{m,t}}, \tag{8}$$

where $\hat{P}_{i,t}$ is the load of node i at moment t. For the degree of node overvoltage, combined with the node load weights, the overvoltage offset indicator of the whole network is finally calculated; the Shapley value method is used to calculate the impact of each node voltage indicator. Each node Shapley value calculation formula is:

$$\begin{aligned} \mu_{i,t} &= \sum_{C \in K} (C)[\mathrm{LVDI}_t(C) - \mathrm{LVDI}_t(C \backslash \{i\})] \\ \nu_{i,t}(C) &= \frac{[(|C|-1)!\,(|K|-|C|)]}{|K|!} \end{aligned}, \tag{9}$$

where: $\mu_{i,t}$ is the Shapley value of distributed PV subject i at moment t; C is the cluster division containing node i; $\nu_{i,t}(C)$ is the weight value that node i occupies in cluster C at moment t; $\mathrm{LVDI}_t(C)$ is the detailed indicator of overvoltage generated by cluster C at power backward; $\mathrm{LVDI}_t(Ci)$ is the overvoltage indicator after removing node i; K is the set of all PV points generating overvoltage; and $|C|$, $|K|$ are the numbers of elements in the set C and K.

The specific node Shapley value is calculated and the value is applied to calculate the specific overvoltage responsibility share size for each corresponding node [23]. The specific responsibility percentage is:

$$R_{i,t} = \frac{\mu_{i,t}}{\sum_{i \in K} \mu_{i,t}} \times 100\%, \tag{10}$$

where $R_{i,t}$ is the specific overvoltage liability value of node i at moment t.

Overvoltage problems can be effectively mitigated in a timely manner through reactive power compensation and active curtailment strategies tailored for distributed PV systems [24]. On a per-distribution line basis, overvoltage incidents are addressed through in-situ prevention measures. As voltage readings near predetermined upper and lower thresholds, proactive steps are implemented to either absorb or supply reactive power. The precise adjustment of reactive power is dictated by the voltage level at the current control node, as illustrated in Fig. 2.

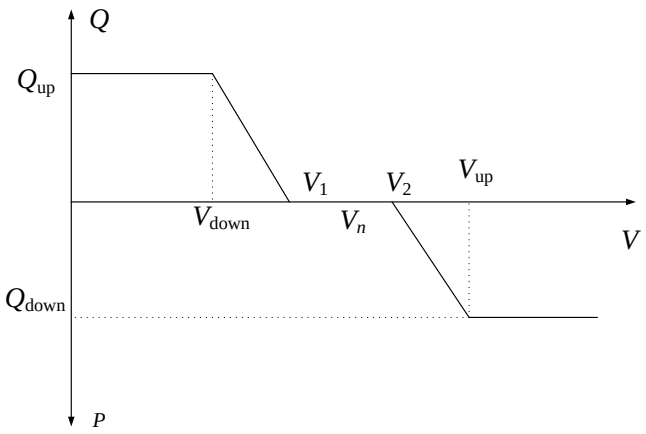

Fig. 2. Q–V dynamically regulated PV power curve

In the figure, Q_{up} is the upper limit of the reactive power margin, which is related to the PV capacity and power factor; V_{up} and V_{down} are the upper and lower limits of the node voltage, and V_1, V_2 are the critical values for controlling the power compensation. Then the Q–V curve obtained on the basis of the current node voltage measurement data is the dynamic regulation of PV power process.

2.3. Control cluster unit division

This paper primarily focuses on coordinating communication connections between different clusters, with node power to node voltage sensitivity serving as the main reference. Partitioning is based on the degree of node coupling within the cluster being high, while the coupling between partitions is relatively weak, as determined by voltage sensitivity.

The voltage control is dominated by voltage sensitivity between nodes and decoupling of active/reactive power of the system based on trend calculation. The active/reactive power sensitivity to voltage is derived from the Jacobi matrix calculated by the Niu La method [23].

$$\begin{bmatrix} \Delta P \\ \Delta Q \end{bmatrix} = \begin{bmatrix} D_{P\theta} & D_{PU} \\ D_{Q\theta} & D_{QU} \end{bmatrix} \begin{bmatrix} \Delta\delta \\ \Delta U \end{bmatrix}, \tag{11}$$

where: ΔP, ΔQ represent the node active and reactive power change; $\Delta\delta$, ΔU are the node voltage phase angle and amplitude change; $D_{P\theta}$, D_{PU}, $D_{Q\theta}$, and D_{QU} belong to the Jacobi matrix elements in the equation that indicates the relationship between the node power and voltage changes; the above formula is transformed into

$$\begin{bmatrix} \Delta\delta \\ \Delta U \end{bmatrix} = \begin{bmatrix} M_{P\theta} & M_{Q\theta} \\ M_{PU} & M_{QU} \end{bmatrix} \begin{bmatrix} \Delta P \\ \Delta Q \end{bmatrix}, \tag{12}$$

where: $M_{P\theta}$ and $M_{Q\theta}$ represent the node active and reactive power regulation after the phase angle change; M_{PU}, and M_{QU} stand for the corresponding change in power after the degree of change in voltage amplitude. The above two formulas are derived from the entire distribution line in a node voltage amplitude and active and reactive power to change the amount of the following relationship between the existence of the formula.

$$\Delta U = M_{PU}\Delta P + M_{QU}\Delta Q. \tag{13}$$

From Eqs. (12) and (13), it can be seen that when one of the active and reactive powers is determined constant while the other is changed, the change in voltage magnitude is only related to the corresponding sensitivity matrix. Therefore, decoupling control of active and reactive power is possible. With the modular indicator function proposed by Louvain's algorithm [24], the corresponding indicators judge the quality of cluster division partition, reduce human interference factors, and electrify indicators such as node edge power, node coupling degree, and so on, for

complex network decomposition. The modularity function can be expressed as:

$$\begin{gathered}\rho = \frac{1}{2m}\sum_i\sum_i\left(A_{ij} - \frac{k_i k_j}{2m}\right)\delta(i,j), \\ m = \frac{1}{2}\sum_i\sum_i A_{ij} \\ \delta(i,j) = \begin{cases} 1 & i,j \text{ located in the same cluster} \\ 0 & \text{other} \end{cases},\end{gathered} \tag{14}$$

where: A_{ij} is the connection edge weight between ij two nodes, directly connected $A_{ij} = 1$, otherwise $A_{ij} = 0$; k_i is the sum of the weights of all nodes connected to i node, and $m = \frac{1}{2}\sum_i\sum_i A_{ij}$ is the sum of all the values of the whole network. The ρ value belongs to the penalty function adjustment, and its size reflects the performance of the division between the corresponding clusters.

During cluster partitioning, it's essential to assess the quality of the resulting partitions while minimizing human interference factors. Complex network decomposition is conducted using electrification metrics such as node edge weights and degree of node coupling [25]. The number of clusters directly impacts the control efficacy of the entire line, and the modular function is employed to gauge the performance of division among corresponding clusters. Additionally, the Sum of Squared Errors (SSE) is utilized to ascertain the optimal number of clusters and evaluate the distance between nodes and cluster centers within each cluster, as expressed in Eq. (15):

$$\mathrm{SSE} = \sum_{i=1}^{E}\sum_{j=1}^{|C_i|} L^2_{j\varepsilon_i}, \tag{15}$$

where $L_{j\varepsilon_i}$ is the electrical distance of node j from the cluster center ε_i. $|C_i|$ is the number of nodes in cluster i. E is the number of cluster divisions. There is a negative correlation between the number of cluster divisions and the number of nodes in the cluster, but it is not a linear relationship. Therefore, according to the corresponding wiring circuit topology to calculate a reasonable index choose the appropriate division of clusters.

In this paper, the sensitivity matrix is initially computed. Based on the sensitivity values, k-means clustering division is conducted. Since k-means division relies on distance, the calculation of distances in the node sensitivity matrix is performed. However, the outcomes of the K-means algorithm are often influenced by the selection of the initial point. An improper selection of the initial point may lead to convergence to a local optimal solution, rather than the global optimal solution. In the classical K-means algorithm, the initial point is randomly chosen, potentially resulting in different outcomes for each cluster division. To overcome these shortcomings, this paper specifies the initial cluster centers based on the calculation results of responsibility sharing. This approach aims to avoid unstable division results and escape local optima. Subsequently, multiple iterations are conducted to refine the clustering.

3. DMPC distributed predictive control algorithm

To achieve the objective of group-weighted consistency, this paper introduces new virtual decoupling control variables denoted as u and a weighting matrix W to the consistency algorithm [21] This enhancement is based on the improved model equation as follows:

$$x(k+1) = Mx(k) + W^{-1}u(k). \tag{16}$$

An enhancement to the aforementioned equation can be achieved by incorporating the current state $x(k)$ of the system to predict the future $x(k+1)$. By default, the current moment is denoted as k, the prediction time domain is denoted as N_p, and the control time domain is denoted as N_c, where $N_p \geq N_c$; The variables $u(k)$ outside the control time domain N_c remain unchanged. With the addition of the virtual control volume to the basic algorithmic model, distributed PV grid-connected systems containing multiple inverter controls can mitigate the impact of a single controller failure or abnormal data, ensuring system-wide control stability. Under the same parameter model conditions, the enhanced model demonstrates improved convergence speed.

To detail the coupling between subsystems, the diagonal element M_{ij} of matrix M is the state transfer term, and the non-diagonal element M_{ij} is the dynamic coupling term. When $M_{ij} \neq 0$ it means that ij is a coupling between the two subsystems, otherwise it means that there is no effect, and Eq. (18) is decomposed into the lower order subsystem form as:

$$x(k+1) = M_{ii}x_i(k) + \sum_{j \in N_i} M_{ii}x_i(k) + w_i^{-1}u_i(k), \tag{17}$$

where N_i is the set of neighboring subsystems to subsystem i. There, the state coupling term $x_i(k)$ exists since the matrix M is a non-diagonal matrix. Taking the state variables of system i at the current moment k as inputs, one can predict the future state information of this system at the $k+1-k+N_p$ moments.

$$X_i(k) = F_i x_i(k) + G_i U_i(k) + \sum_{j \in N_i} H_{iJ} X_i(k), \tag{18}$$

where $X_i(k)$ is the state prediction matrix and $U_i(k)$ is the input matrix. The form of each term in the equation is as follows:

$$X_i(k) = \begin{bmatrix} x_i(k+1 \mid k) \\ x_i(k+1 \mid k) \\ \vdots \\ x_i(k+1 \mid k) \end{bmatrix}, U_i(k) = \begin{bmatrix} u_i k \\ u_i(k+1) \\ \vdots \\ u_i(k+N_c-1) \end{bmatrix}, \quad F_i = \left[M_{ij}, M_{ij}^2, \cdots M_{ij}^{N_p} \right]^T,$$

$$G_i = \begin{bmatrix} w_i^{-1} & 0 & 0 & 0 \\ M_{ii}w_i^{-1} & w_i^{-1} & \cdots & 0 \\ \vdots & \vdots & \ddots & \vdots \\ M_{ii}^{N_P-1}w_i^{-1} & M_{ii}^{N_P-2}w_i^{-1} & \cdots & \sum_{c=0}^{N_P-N_C} M_{ii}^c w_i^{-1} \end{bmatrix},$$

$$H_{ij} = \begin{bmatrix} M_{ii} & 0 & 0 & 0 \\ M_{ii}M_{ij} & M_{ii} & \cdots & 0 \\ \vdots & \vdots & \ddots & \vdots \\ M_{ii}^{N_P-1}M_{ij} & M_{ii}^{N_P-2}M_{ij} & \cdots & M_{ij} \end{bmatrix},$$

where $X_i(k)$ as a vector, is the prediction matrix prediction state quantity, in this case a physical quantity related to power. The F_i matrix is the vector of coupled state matrices; the G_i matrix is the decoupled control variable and coupled state product matrix, a lower-triangular matrix; H_i is the lower-triangular coupled state matrix as a multiplicative product of the input vector and the coupled state matrix.

In the distributed PV grid-connected system based on cluster partitioning, different neighboring groups require communication connections. However, under the algorithm in Eq. (12), after completing a communication, the prediction model of adjacent subsystems cannot be obtained. Consequently, the predicted quantities $x_j(k+m)$ for subsystem i at that moment of coupling cannot be acquired. To address this issue, an approximation is employed, replacing the predicted state quantities with the state quantities at the k moment, thereby simplifying to:

$$X_j(k) = x_i(k)I_{N_P}, \tag{19}$$

where I_{N_P} is the column vector of order 1 with all elements of order 1.

The objective function for optimization is determined by taking the difference between the output state vector and the state reference, and combining it with the associated weight matrix. The minimum value is then selected.

$$\min J_i(k) = \|X_i(k) - C_i(k)\|_Q^2 + \|U_i(k)\|_R^2, \tag{20}$$

where $Q = qI_{N_P}$ and $R = rI_{N_P}$ are the weight matrices, and reference values of the state vector, respectively, which can be calculated by the following expression:

$$C_i(k) = \frac{\sum\limits_{j \in N_i \cup \{i\}} w_j(k)x_j(k)}{\sum\limits_{j \in N_i \cup \{i\}} w_j(k)} I_{N_P}, \tag{21}$$

where $N_i(k) \cup \{i\}$ is the set of current and neighboring subsystems.

To minimize the objective function, the input variables in the objective function are derived and made to be 0. The inputs to the optimal control can be calculated and corrected in the optimal control, the main formula is:

$$\hat{u} = \sum_{j \in N_i} a_{ij}(u_i(k) - u_i(k)). \tag{22}$$

In the derivation of the DMPC algorithm above, only the information from the requested subsystem and its nearby neighboring cluster systems is utilized. This, combined with the actual coupling state information of the subsystems, helps in selecting the appropriate optimized objective function. This function considers the relationship between the output state vector and the state reference quantity, forming a type of distributed control algorithm. The actual computational algorithm calculation flow is shown in Fig. 3.

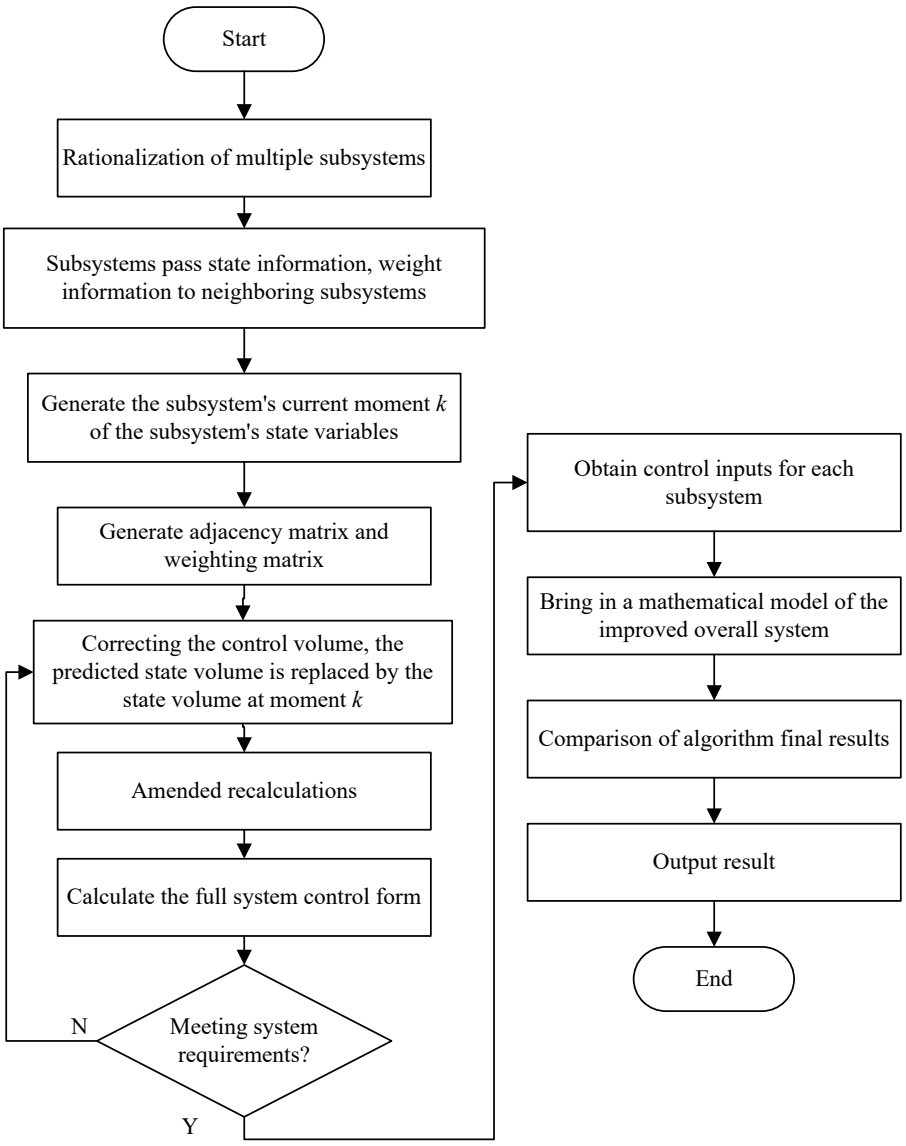

Fig. 3. Flowchart of DMPC algorithm

4. Simulation example analysis and discussion

Since distributed PV grid-connected overvoltage typically occurs between 10:00 and 16:00, this paper focuses on verifying the control effectiveness during this time period. To achieve this, the 10 kV distribution line data and wiring topology of the Dingxi area in Gansu Province are combined with the IEEE 33-node model for simulation. The region experiences annual sunshine

hours between 2240 and 2500 hours, with an average daily sunshine duration of more than 6 hours. The annual solar exposure ranges from 5260 to 5910 MJ/m². The validated data is from the distribution line data of Dingxi, Gansu Province, on September 13, 2023. The environmental conditions on that day were: sunny during the day; temperatures ranging from 9°C to 26°C; a light exposure of 15.5 MJ/m²; AQI of 30; and southerly winds at level 2. This data is used to verify the effectiveness of the proposed cluster division and DMPC algorithm control for overvoltage regulation in distributed energy distribution networks. The final example is shown in Fig. 4.

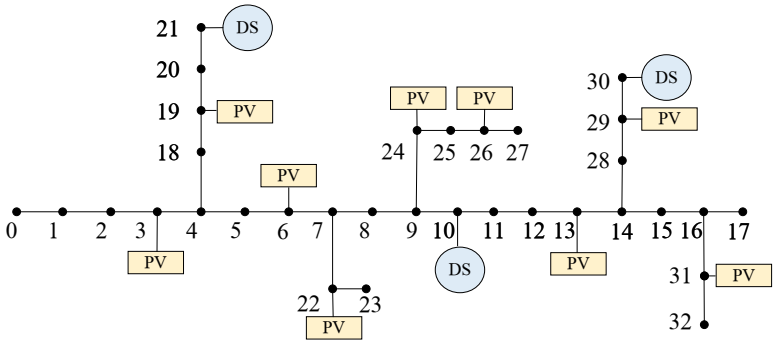

Fig. 4. Calculation system diagram

In the example, node 0 serves as the system substation connection point. There are a total of eight distributed PV access points, located at nodes 3, 6, 13, 19, 22, 24, 26, and 29. Additionally, energy storage devices are connected at nodes 10, 21, and 30. The 24-hour output curves of the distributed energy at each node are shown in Fig. 5.

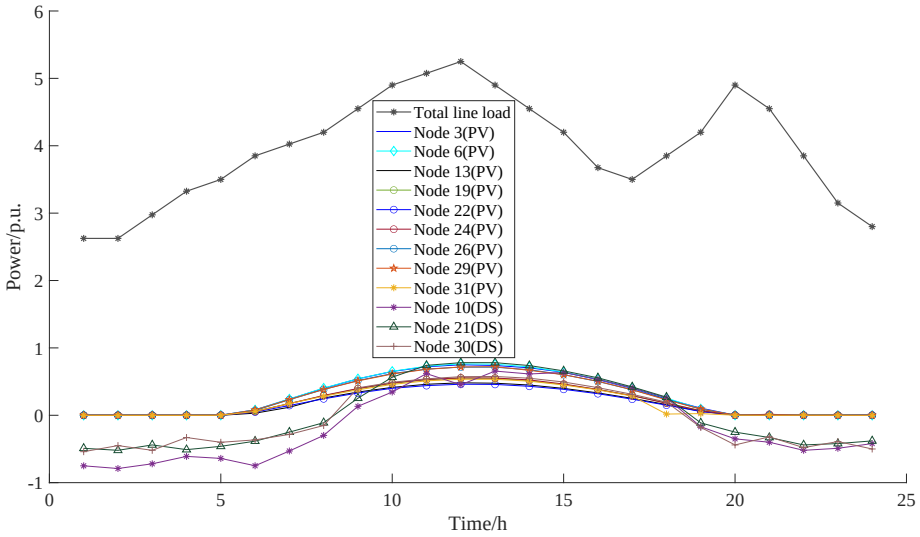

Fig. 5. Power curve at each node and PV point curve

4.1. Cluster segmentation results

Using the point in time of maximum total load in the load profile as a reference, the responsibility sharing and clustering algorithms mentioned in Section 3 are applied to cluster the remaining nodes, excluding those connected to the substation. The responsibility calculation data and system parameters at that time are used to compute the Jacobian matrix for active-reactive decoupling. The corresponding weight matrix is generated by combining the electrical distance parameters. The electrical distance of each node from node 0 is shown in Fig. 6.

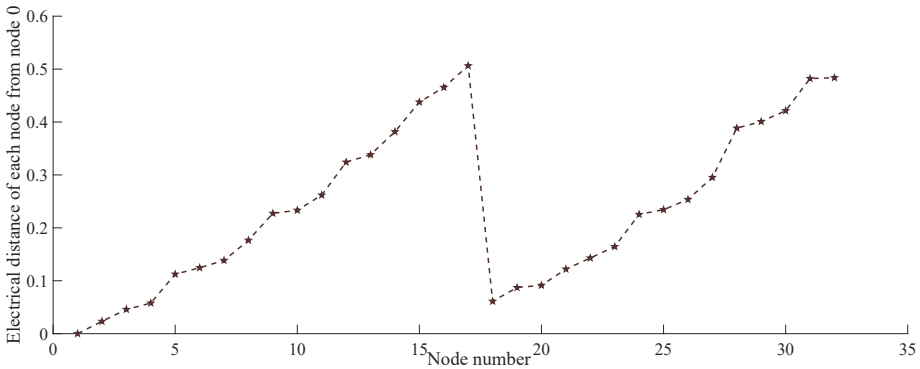

Fig. 6. Electrical distance between each node and node 0

Based on the electrical distance, the proposed algorithm divides the nodes into clusters. A reasonable number of cluster divisions is determined to be 6, according to the elbow rule. The resultant index of cluster divisions for the corresponding K-value is shown in Fig. 7 as follows:

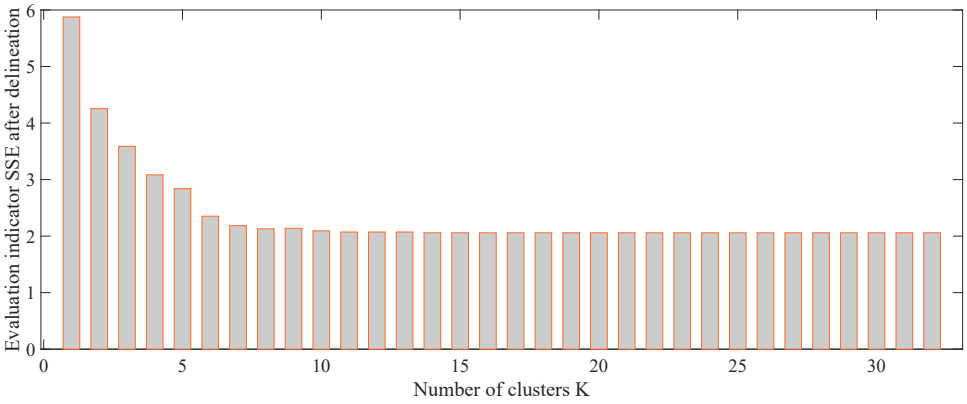

Fig. 7. Map of cluster division metrics

The results of the optimal division when K is chosen to be 6 are shown in Table 1. The corresponding system division result is shown in Fig. 8 Node cluster division diagram.

Table 1. Node cluster division table

Cluster number	Node number
1	1, 2, 3, 4, 18, 19, 20, 21
2	5, 6, 7, 22, 23
3	8, 9, 24, 25, 26, 27
4	10, 11, 12, 13
5	14, 15, 28, 29, 30
6	16, 17, 31, 32

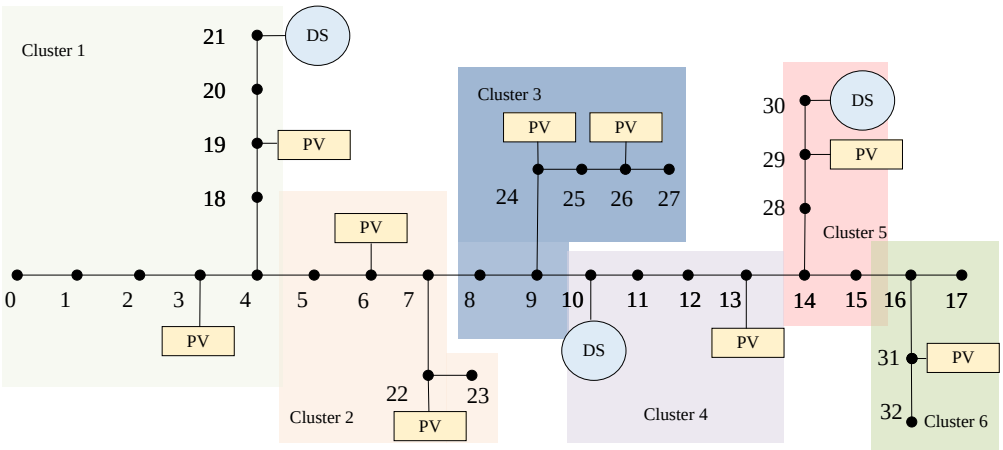

Fig. 8. Node cluster partitioning diagram

4.2. Verification of final voltage regulation results

Figure 9 shows that integrating a large number of PV points in the distribution line causes the voltage of the entire line to rise above 1.07 p.u.

Specifically, the PV access points at nodes 24 and 26, due to their close electrical proximity, result in a significant voltage rise near these nodes, with overvoltages approaching 1.08 p.u. Conversely, the 10th node does not experience overvoltage issues, even when the PV output causes overvoltage along the whole line, because of the energy storage equipment configured at this node. This outcome is observed in both the final experiment and conventional simulations. The cluster division distributed predictive control strategy, however, demonstrates a more ideal control effect on distribution line overvoltage. It effectively reduces voltage volatility across the entire distribution line, particularly evident in node 26 where the reduction is nearly 9%. The regulation effect is significant.

Based on the distribution line data, trend calculations are performed for the networks both without and with distributed PV added. This is done to verify the overvoltage situation on the distribution lines and confirm the actual impact of distributed PV on grid-connected voltage.

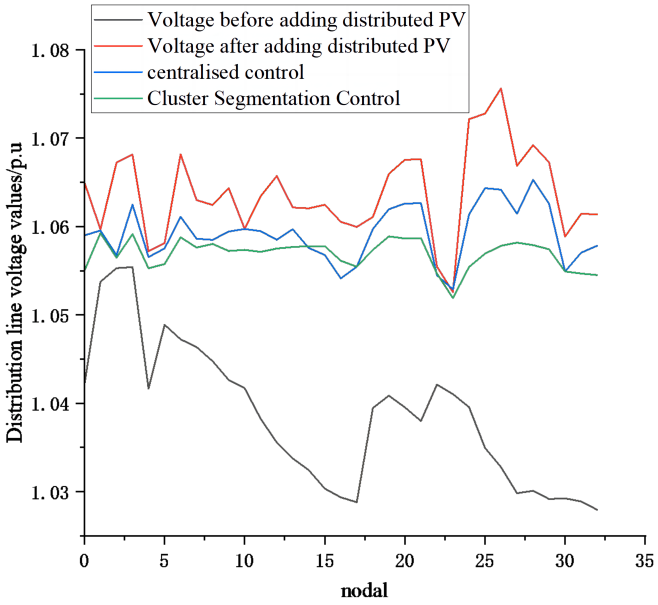

Fig. 9. Control results validation chart

According to the Chinese national standard *GB/T12325*, the voltage deviation at a three-phase common connection point of 20 kV and below should not exceed +7% of the nominal voltage. Therefore, a voltage regulation value of 1.06 is utilized. From Fig. 9 it is evident that with the addition of distributed PV, the voltage across the entire system increases significantly, leading to an overvoltage situation along the entire line. Nodes 24 and 26 experience particularly severe overvoltage issues with cluster 3 showing the most serious overvoltage among all the clusters.

5. Comparative validation and discussion of results

To verify the effectiveness of the control strategy presented in this paper, we have conducted a comparative analysis that includes not only the traditional centralized control model but also two additional methods: neural network predictive control, as mentioned in Reference [16], and the non-cooperative subsystem autonomy model [26].

The traditional centralised control model is based on unified scheduling by the power sector and autonomous operation of the subsystems, where each controller responds to real-time outputs and self-optimizes according to basic constraints;

The strategy proposed in Reference [16] includes deep neural networks utilized to predict solar PV power generation and electricity load. They adjust the electricity load based on the difference between the two, thereby improving the utilization rate of PV power generation.

In the non-cooperative subsystem autonomy model, the model aims to increase on-site PV power consumption and thereby reduce the impact on the main grid. This is achieved by introducing a feed-in tariff that is lower than the electricity price. To maximize local PV consumption capacity, the initial value of the feed-in tariff is set to zero in this model.

As shown in Fig. 10 in the traditional centralized control mode, due to the distributed PV grid connection, the field data from 11:00 to 15:00 during periods of serious over-voltage show that the actual site exceeds the highest national regulation standards by more than 7%. Consequently, the grid connection must be disconnected from the power supply, ensuring that the maximum voltage remains at approximately 1.07 P.U.

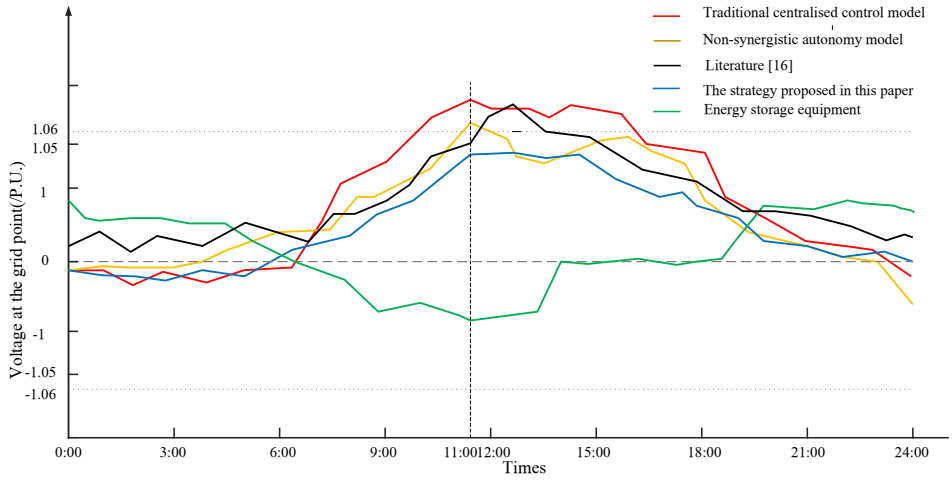

Fig. 10. Control results validation chart

After coordinated control in non-cooperative autonomous mode, the main transformer was able to regulate the voltage overload within the subsystem to a certain extent. During this period, the output power of the main inverter was observed to maximize profit. However, the lack of coordination between the subsystems and the limited regulation capacity still resulted in a maximum value exceeding 1.06 P.U., which did not fully exploit the entire consumption capacity.

The strategy proposed in Reference [16] is able to provide a certain degree of overvoltage mitigation based on the predicted values, but the amount of data required is huge and the degree of voltage fluctuation at the measurement points is high, resulting in severe network losses.

The strategy proposed in this paper maximizes the use of coordinated autonomy of the subsystems, as well as coordinated communication with neighboring regions. It employs the Shapley value to calculate the responsibility allocation, thereby minimizing the amount of data required for prediction. This approach enables smooth overvoltage mitigation.

The energy storage device discharges during nighttime hours to supplement load requirements and tries to absorb excess energy to prevent over-voltage when the PV system is generating power from 6:00 to 14:00. However, it reaches its capacity limit after 14:00 and can no longer store energy for further mitigation.

To illustrate the economics of the control strategies proposed in this paper and the effectiveness of the algorithms, the three aforementioned strategies are used for comparative validation. Table 2 presents the specific network losses, voltage deviations, power losses, and economic gains under the four control schemes.

Table 2. Comparison of economics under different control methods

Norm	**Traditional centralised control**	**Non-synergistic subsystem autonomy**	**Reference [16]**	**The methodology proposed in this paper**
Network losses/MW	0.1032	0.1005	0.0998	0.0952
Voltage deviation/P.U.	0.65	0.59	0.51	0.47
PV active reduction/MW	1.376	1.324	1.286	1.255
Economic gains/10^3yuan	13.61	14.25	14.66	15.12

The results indicate that real-world communication delays and distortions are considered, as the DMPC controller maintains inter-controller communication with each subsystem, and each subsystem controller performs local optimization for control tasks. Addressing the overvoltage issue, optimal voltage control also reduces network losses, achieving a minimum loss of 0.0952 MW as proposed in this paper. Voltage deviation can be minimized to 0.47 P.U., thereby enhancing voltage stability. Additionally, active power reduction is minimized to 1.255 MW among the four schemes, ensuring optimal economic operation of the entire distribution network. These findings highlight significant improvements in the system's performance for overvoltage control, taking into account communication and computational requirements.

Analytical discussion:

– Simulation and comparative verification demonstrate that the control strategy proposed in this paper addresses the overvoltage issue caused by power back-feeding when distributed PV systems are connected to the grid. It calculates the size of the overvoltage responsibility for each node by combining indicators such as electrical distance with cooperative game theory. By selecting the central responsible node, this approach resolves the challenge of handling large amounts of data required for neural network predictions.
– Grouping the entire distribution system into clusters enables cluster autonomy, maximizing the utilization of each inverter's active and reactive power to regulate voltage capacity. This approach reduces the mechanical action required for transformer regulation, thereby decreasing network losses and increasing economic efficiency.
– If each cluster does not consider communication coordination, it cannot fully mobilize the voltage regulation capability of the entire power system. This paper proposes a cluster-divided DMPC control strategy to ensure communication between each region. This coordinated

approach allows all regions to maximize the use of inverter capacity and effectively mitigate overvoltage issues.

– In contrast, the DMPC-based voltage optimization proposed in this paper maximizes the grid-connected capacity of PV systems while preventing congestion. It also achieves smooth voltage regulation, thereby mitigating system-wide overvoltage issues and maximizing economic benefits.

6. Conclusions

This paper simplifies the data of distributed photovoltaic grid-connected distribution lines in Dingxi, Gansu Province, and constructs the corresponding topological grid structure. The Shapley value method from cooperative game theory is used to calculate the overvoltage responsibility sharing of the nodes. Then, reasonable clusters are divided based on the nodes' electrical distance index. On this basis, all cluster subsystems are coordinated to control the active and reactive power output of the entire distribution line. The optimization objective function is to minimize the combined weight difference between the output state vector and the state reference. Finally, a comparative analysis with the control schemes proposed in recent literature is performed to verify and discuss the advantages and disadvantages of each scheme. The simulation results show that the overvoltage problem of the entire distribution line can be mitigated more effectively under the group-distributed predictive control strategy, improving distributed PV grid-connected access.

The Shapley method used in this paper to calculate the corresponding nodal overvoltage liability can lead to excessive computational complexity. Additionally, selecting the initial cluster division centroid based on a higher liability value may cause the iteration to fall into a local optimal solution. In the current power sector, when the voltage exceeds the national standard by more than 10% without adding energy storage equipment, the only solution might be to manually remove the entire PV node. However, the high cost of energy storage equipment and determining the appropriate capacity for such equipment are issues that this paper does not address.

Recommendations for further research include the installation location and capacity of energy storage equipment that can solve the PV grid-connected overvoltage problem in a specific area. Additionally, the unique volatility and randomness of distributed photovoltaic systems in grid connection will affect the stability of the entire power system. If an accurate model of photovoltaic grid-connected volatility is established and the stability of the PV network is proven, it will enable targeted dissipation of excessive PV active capacity output to address the overvoltage problem. This will be a future research trend for distributed photovoltaic grid connection.

References

[1] http://www.xinhuanet.com/politics/19cpcnc/2017-10/27/c_1121867529.htm, accessed April 2024.

[2] Chai Yuanyuan, *Distributed Voltage Optimization Control for Distribution Networks with High Penetration of Photovoltaics*, PhD Thesis, Tianjin, Tianjin University (2021).

[3] Kaczorowska D., Rezmer J., Janik P., Sikorski T., *Smart control of energy storage system in residential photovoltaic systems for economic and technical efficiency*, Archives of Electrical Engineering, vol. 72, no. 1, pp. 81–102 (2023), DOI: 10.24425/aee.2023.143691.

[4] Zhang X., Ming L., Zixuan G., *A review and outlook on control strategies for new energy grid-connected inverters*, Journal of Global Energy Interconnection, vol. 4, no. 5, pp. 506–515 (2021), DOI: 10.19705/j.cnki.issn2096-5125.2021.05.010.

[5] Jingjing T., Yu Q., Feng Z., Shenglin M., Huaxuan X. *et al.*, *Energy-saving optimal scheduling under multi-mode "source-network-load-storage" combined system in metro station based on modified Gray Wolf Algorithm*, Archives of Electrical Engineering, vol. 73, no. 1, pp. 121–141 (2024), DOI: 10.24425/aee.2024.148861.

[6] Ali Elrayyah, Sozer Yilmaz, Malik Elbuluk *et al.*, *Microgrid-Connected PV-Based Sources: A novel autonomous control method for maintaining maximum powe*, IEEE Industry Applications Magazine, vol. 21, no. 2, pp. 19–29 (2015), DOI: 10.1109/MIAS.2014.2345822.

[7] Liu R., Kuihua W., Liang F. *et al.*, *Coordinated Optimization and Control of Voltage Partitioning in Active Distribution Networks with High Penetration of Distributed Photovoltaics*, Acta Energiae Solaris Sinica, vol. 43, no. 2, pp. 189–197 (2022), DOI: 10.19912/j.0254-0096.tynxb.2020-0239.

[8] Fazio A.R.D., Risi C., Russo M., Santis M.D., *Coordinated Optimization for Zone-Based Voltage Control in Distribution Grids*, IEEE Transactions on Industry Applications, vol. 58, no. 1, pp. 173–18 (2022), DOI: 10.1109/TIA.2021.3129731.

[9] Adhi Kusmantoro, Irna Farikhah, *Solar power and multi-battery for new configuration DC microgrid using centralized control*, Archives of Electrical Engineering, vol. 72, no. 4, pp. 931–950 (2023), DOI: 10.24425/aee.2023.147419.

[10] Iweh Chu D. *et al.*, *Assessment of the optimum location and hosting capacity of distributed solar PV in the southern interconnected grid (SIG) of Cameroon*, International Journal of Sustainable Energy, vol. 43, no. 1 (2024), DOI: 10.1080/14786451.2023.2168002.

[11] Moulum P.A., Mandeng J.J., Kom C.H. *et al.*, *Optimal PMU placement in the Southern Cameroon Interconnected Grid considering the effect of a group of ZIBs for complete obervability and dynamic stability*, Research Square, PREPRINT (Version 1) 2024, DOI: 10.21203/rs.3.rs-3934743/v1.

[12] Ibrahem Mohamed A. Mahmoud *et al.*, *The impact of smart transformer on different radial distribution systems*, Archives of Electrical Engineering, vol. 70, no. 2, pp. 271–283 (2021), DOI: 10.24425/aee.2021.136983.

[13] Zhang G., Yi Y., Xian P., *Overvoltage Control of Photovoltaic Grid-Connected Based on Predictive Model*, Smart Power, vol. 45, no. 9, pp. 20–25 (2017).

[14] Yu M., Zhu J., Yang L., *Short-term load prediction model combining FEW and IHS algorithm*, Archives of Electrical Engineering, vol. 68, no. 4, pp. 907–923 (2019), DOI: 10.24425/aee.2019.130691.

[15] Zhao Y., Zhi W., Zhonghao Q. *et al.*, *Active Distribution Network Distributed Optimization and Scheduling Considering Source-Load Spatio-Temporal Correlation*, Automation of Electric Power Systems, vol. 43, no. 19, pp. 68–76 (2019).

[16] Guozheng H., Shujuan T., Zihan Z., *Load regulation application of university campus based on solar power generation forecasting*, Archives of Electrical Engineering, vol. 72, no. 2, pp. 429–441 (2023), DOI: 10.24425/aee.2023.145418.

[17] Chai Yuanyuan, Yixin Liu, Chengshan Wang *et al.*, *Voltage Coordination Control for Distributed Photovoltaic Generation Clusters with Incomplete Measurements*, Proceedings of the CSEE, vol. 39, no. 8, pp. 2202–2212+3 (2019), DOI: 10.13334/j.0258-8013.pcsee.182485.

[18] Biserica M., Foggia G., Chanz E., Passelergue J.C., *Network partition for coordinated control in active distribution networks*, 2013 IEEE Grenoble Conference, Grenoble, France, pp. 1–5 (2013), DOI: 10.1109/PTC.2013.6652277.

[19] Li L., Junxi W., Yi H. *et al.*, *Day-Ahead Allocation Planning of Multi-Point PV-DG Based on K-means Clustering Particle Swarm Algorithm*, High Voltage Engineering, vol. 43, no. 4, pp. 1263–1270 (2017), DOI: 10.13336/j.1003-6520.hve.20170328025.

[20] Song B., Seol H., Park Y., *A patent portfolio-based approach for assessing potential R&D partners: An application of the Shapley value*, Technological Forecasting and Social Change, vol. 103, no. 165, pp. 156–165 (2016), DOI: 10.1016/j.techfore.2015.10.010.

[21] Reddy P.V., Shevkoplyas E., Zaccour G., *Time-consistent Shapley value for games played over event trees*, Automatica (Journal of IFAC), vol. 49, no. 6, pp. 1521–1527 (2013).

[22] Tole Sut., Arsyad Cahya S., Giovanni P., Awang J., Kashif I., *Maximum power point tracking techniques for low-cost solar photovoltaic applications – Part II: Mathematical Calculation and Measurement and Comparison, criteria on choices and suitable MPPT techniques*, Archives of Electrical Engineering, vol. 72, no. 2, pp. 299–322 (2023), DOI: 10.24425/aee.2023.145410.

[23] Ying Chen, Chen Shen, *A Jacobian-free Newton-GMRES(m) method with adaptive preconditioner and its application for power flow calculations*, IEEE Transactions on Power Systems, vol. 21, no. 3, pp. 1096–1103 (2006), DOI: 10.1109/TPWRS.2006.876696.

[24] Santosh Kumar Gupta, Jayant Tripathi, Mrinal Ranjan, Ravi Kumar Gupta *et al.*, *Maximization of injected power and efficiency based optimal location of DPFC using iterative procedure*, Archives of Electrical Engineering, vol. 71, no. 1, pp. 91–108 (2022), DOI: 10.24425/aee.2022.140199.

[25] Olfati-Saber R., Fax J.A., Murray R.M., *Consensus and Cooperation in Networked Multi-Agent Systems*, Proceedings of the IEEE, vol. 95, no. 1, pp. 215–233 (2007), DOI: 10.1109/JPROC.2006.887293.

[26] Reshikeshan S.S.M., Matthiesen S.L., Illindala M.S. *et al.*, *Autonomous Voltage Regulation by Distributed PV Inverters with Minimal Inter-node Interference*, IEEE Transactions on Industry Applications, vol. 57, no. 3, pp. 2058–2066 (2021), DOI: 10.1109/TIA.2021.3064911.